ISSN 1392–1320 MATERIALS SCIENCE (MEDŽIAGOTYRA). Vol. 30, No. 1. 2024

Experimental Determination of a Strain State in a Bulk Forming of a Low Carbon Steel

Plavka SKAKUN [1], Dragan RAJNOVIC [1] *, Petar JANJATOVIC [1], Dejan MOVRIN [1], Miroslav DRAMICANIN [1], Lucijano BERUS [2], Mirko FICKO [2]

[1] *Department for Production Engineering, Faculty of Technical Science, University of Novi Sad, Trg Dositeja Obradovica 6, 21000 Novi Sad, Serbia*
[2] *Faculty of Mechanical Engineering, University of Maribor, Smetanova ulica 17, 2000 Maribor, Slovenia*

http://doi.org/10.5755/j02.ms.34605

Received 24 July 2023; accepted 22 September 2023

An experimental metallographic method for determining strain distribution in a cold formed workpiece is presented in this paper. The method, based on the dependence of recrystallized grain size on prior deformation, was applied to a bulk formed element made of low carbon steel. Strain distribution was obtained by the calibration curve which gives the relation between recrystallized grain size and prior deformation. To determine strain values, the average grain size was measured in the longitudinal cross-section of the formed element. To accurately differentiate deformation zones, additional observation of carbides and nonmetallic inclusions morphology was utilized, also. The grain size and strain noticeably differ through the cross-section. It is observed that in the middle part, material flows freely through the die opening without significant deformation. From this zone, strain increases gradually, reaching the highest value at the contact surface of the die slope, while the top part flows radially having intermediate values of strain.
Keywords: strain value, bulk metal forming, low carbon steel, grain size, metallography.

1. INTRODUCTION

Distribution and values of strain within a workpiece obtained by a metal forming are of great importance in a production process design. Insight into the strain distribution shows the way material flows during forming operation, zones of critical high strain values, and also helps in stress state determination.

Nowadays numerical simulations are the prevailing tool both in strain and stress determination, providing results in a relatively short time with good accuracy [1 – 6]. Compared to numerical simulations, experimental methods usually require longer and more demanding procedures. However, the obtained results are more accurate showing true strain values in a formed workpiece.

Experimental methods for strain state determination are not numerous. One approach is based on the results of hardness or micro-hardness measurement. It is possible to obtain values of strains within a workpiece through the hardness-strain relation [7 – 9]. To apply this method, it is necessary to determine the hardness-strain relation for specific material and later through hardness measurement to obtain strain values. If the stress-strain curve is determined through conventional ways (e.g. uniaxial tension or compression), a relation between stress and hardness also can be made. On the other hand, the hardness-strength relation [10, 11], or hardness to flow stress relation could also be used [5, 12]. In this case, strain values could be determined through the flow curve.

Another experimental method for strain state determination is the digital image correlation technique (DIC) [13 – 16]. Digital image correlation is a method for strain and displacement measuring which is based on non-contact optical technique. Because it is based on observation of surface geometry, through this method only data related to strains on the workpiece surface can be obtained. In metal forming it is usually used for the determination of sheet metal characteristics.

A strain state within a bulk formed workpiece can also be determined through an experimental method based on the relation between recrystallized grain size and prior deformation. Although this method requires metallographic material preparation, determination of calibration curve, and grain size measurement for different strain values, it gives valuable data on strains within the workpiece volume. Also, the way that material flows through the forming process could be observed. Determination of the strain state of the cold formed parts made of pure aluminium by this method is presented in [17, 18]. In those cases, when single phase material is formed, the flow of material is uniform and there are no additional constraints of grain deformation. Thus, measurement of the grain size could be easily accomplished. However, if a material consists of several phases or has a complex microstructure the measurement of grain size is more challenging. Furthermore, different phases or microstructures additionally influence the deformation of a single grain due to the different mechanical properties of every crystal.

For that reason, in this paper, the proposed experimental method was applied for strain state determination of the bulk formed element of low carbon steel, which consists of two micro-constituents, i.e. ferrite and pearlite. In that way, the

* Corresponding author. Tel.: +385-21-4852338; fax: +385-21-454495.
E-mail: *draganr@uns.ac.rs* (D. Rajnovic)

applicability of the method is tested for multiphase microstructures and the strain state in a material volume is determined.

2. MATERIALS AND METHODS

The material analyzed in this study was a low carbon steel C10 (EN 10277-2:2008), in the form of a bar. The chemical composition of the steel was: 0.123 % C, 0.165 % Si, 0.504 % Mn, 0.012 % P, 0.038 % S, 0.131 % Cr, 0.19 %Ni, 0.004 % Mo, 0.003 % V, and balance Fe.

All specimens were heat treated equally to attain the same initial microstructure. That is, all specimens were first soft annealed at 700 °C for 3.5 h and then slowly cooled at 30 °C/h to 550 °C. After that, the specimens were air cooled to room temperature.

Accordingly, the uniform undeformed microstructure consisted of ferritic grains with average size d_{av} = 18 ± 0.8 μm and some strings of localized spheroidal carbides were obtained, as illustrated in Fig. 1.

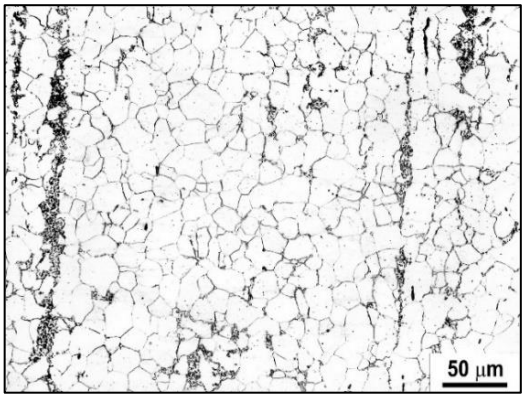

Fig. 1. Starting microstructure of the used steel C10

To obtain the calibration curve, which gives a relationship between the recrystallized grain size and the strain values, the upsetting of cylindrical steel billets was performed with a true strain φ between 0.1 and 1.15, in 9 steps. The uniform strain distribution through the specimen was accomplished by the elimination of contact friction by using Teflon foil. In this way, a uniaxial stress state was attained in specimens. Following upsetting each deformed cylinder was heat treated at 690 °C for 5 hours with slow cooling in a furnace to achieve the recrystallization of grains. After that, the metallographic examination and grain size measurement were done (described later). Furthermore, the results of this experiment (calibration curve) could be used for the additional determination of the flow curve and corresponding stress state.

The tool used in the extrusion experiment consisted of a forward extrusion die and a flat punch. The starting cylindrical billet (30 mm diameter and 38.5 mm height, Fig. 2) was placed into the die, and it was pressed downwards by the punch (15 mm stroke). In this way, the material could flow in two directions – axially into the extrusion die and radially as in the upsetting; resulting in divided material flow. The tool was mounted on the hydraulic press Sack & Kiesselbach (F_{max} = 6.3 MN). After the forming process, the extruded element was also heat treated at 690 °C for 5 hours to get new recrystallized grains. The metallographic examination was performed at the longitudinal half-section of the element.

Fig. 2. The starting billet and the extruded element

The metallographic examinations for all specimens were done after the standard metallographic preparation: SiC papers grinding (grid from 220 up to 2500); and diamond suspension polishing (diamond grain size 6, 3, 1 and ¼ μm). The grains were revealed by etching with 3 % nitric acid solution in alcohol (3 % Nital). All specimens were examined with an Orthoplan (Leitz, Germany) light microscope.

In addition to a qualitative analysis of a microstructure, a quantitative analysis of the apparent grain size according to procedure EN ISO 643:2019 was done. To obtain the apparent grain size, a planimetric method was used. The measurements were performed within a circle of appropriate size (usually between 150 and 500 μm) containing around 100 grains. Subsequently, the mean diameter of grains (d) was calculated and reported. If the two microconstituents are present in a material (as ferrite grains and pearlite islands) the grain size measurements must be done by counting both constituents. Also, the procedure EN ISO 643:2019 could be applied for ferrite/pearlite steels up to 0.25 % carbon content. In this study, in the starting microstructure both ferrite grains and islands of spheroidal carbides were present and were used for measurements. However, after the deformation of samples, the localized carbide islands disappeared as carbides became scattered in the matrix due to material flow. Regarding that, there were no longer carbide islands that could be counted as grains. The described procedure was used for the measurement of grain size for the calibration curve (at 5 fields of view), and also for grain size measurement in the characteristic zones on the longitudinal cross-section of the extruded element.

3. RESULTS AND DISCUSSION

3.1. Calibration curve

The calibration curve, i.e. correlation of the mean grain diameter to the applied strain, is presented in Fig. 3. This correlation is approximated by the power Eq. 1 with a coefficient of determination R^2=0.9566:

$$\varphi = 35.321 \cdot d^{-1.411}, \quad (1)$$

where φ is the true strain; d is the grain diameter in μm.

The number and size of recrystallized grains depend on the amount of applied deformation before recrystallization. The small number of grains (large grains diameter) is attained for the small amount of deformation. On the other hand, higher amounts of deformation accumulate more

energy in the sample and thus produce a large number of small size grains after recrystallization. Furthermore, a minimum of accumulated deformation energy must be achieved for recrystallization to start.

The characteristic micrograph of different size grains obtained for different amounts of strain are shown in Fig. 4. With the increase of strain, the ferrite grain size decreases after recrystallization, while spheroidal carbides remain unaffected by heat treatment. However, due to increased deformation the spheroidal carbides become more dispersed in the microstructure and are not grouped anymore in islands compared to the starting microstructure (see Fig. 1). Thus, the material flow could be observed from the dispersion and movement of carbides.

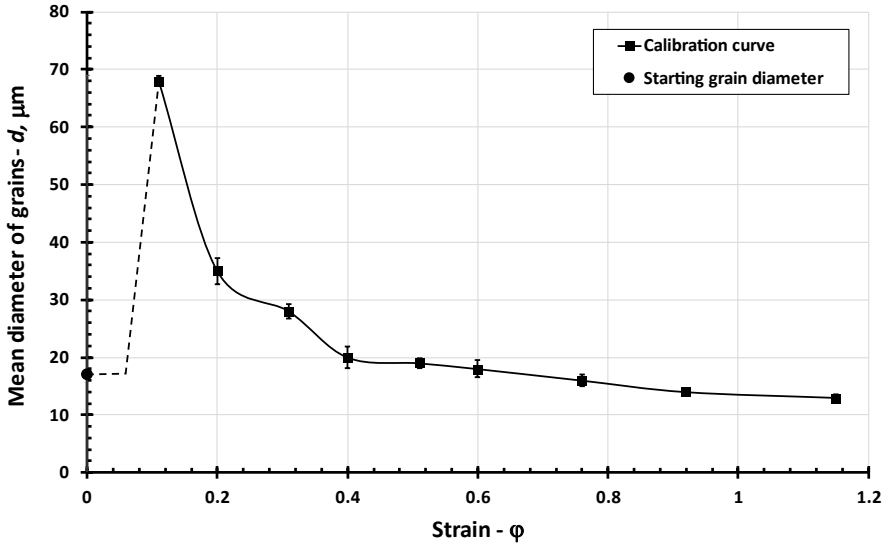

Fig. 3. Calibration curve – grain diameter vs. strain

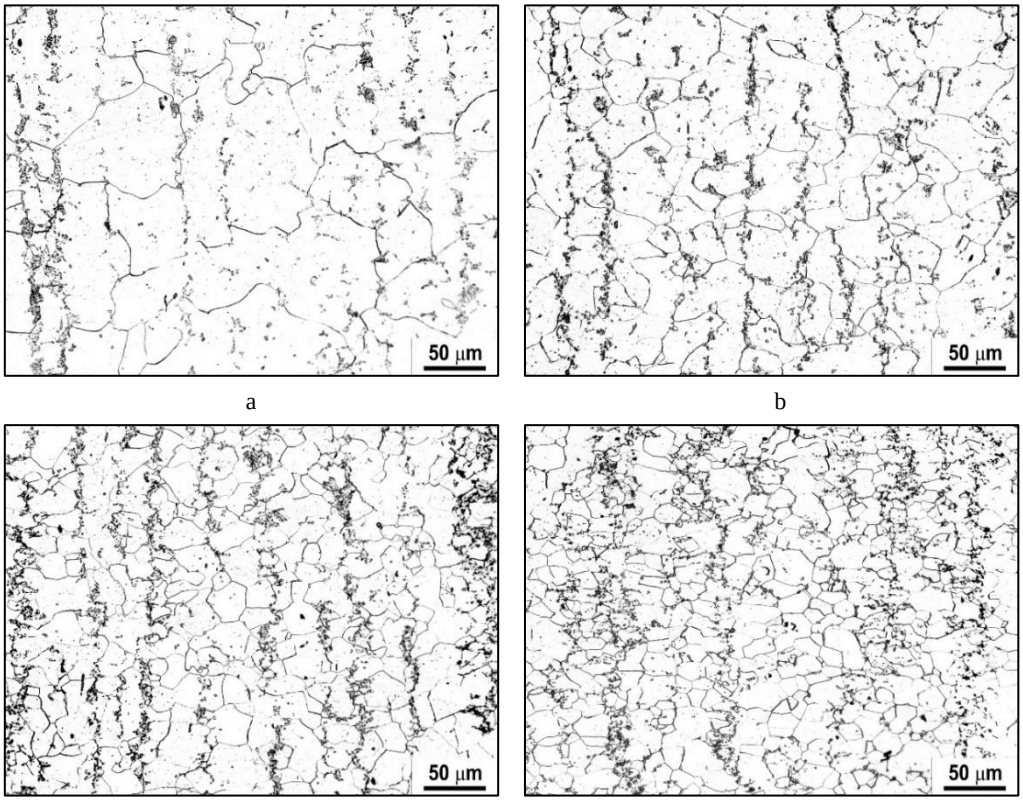

Fig. 4. The microstructures for different strain values: a – φ = 0.11; b – φ = 0.2; c – φ = 0.4; d – φ = 1.15

3.2. Macro and microstructure of the extruded element

The macrostructure of the longitudinal half-section of the extruded element is presented in Fig. 5 a. It can be seen that the distribution of grain size is not uniform (Fig. 5 a, zones I to IV). The corresponding results of measurement of the average grain size are presented graphically in Fig. 5 b (the positions of measurement are represented with black dots). The average diameter of grain varies from 14 to 132 μm, thus revealing different strain zones. In the lower central part (zone I), which is extruded at the beginning of the process, the grain size is approximately around the starting grain size of 17 – 19 μm. In zone II, the grains adjacent to zone I are the largest, around 100 μm. Moving away from the boundary with zone I, the grain diameter decreases to values around 30 μm. In the upper part of the extruded element (zone III) the grains have a diameter between 20 and 30 μm. The smallest grains are present in zone IV, near the slope of the die, and have values between 14 and 20 μm.

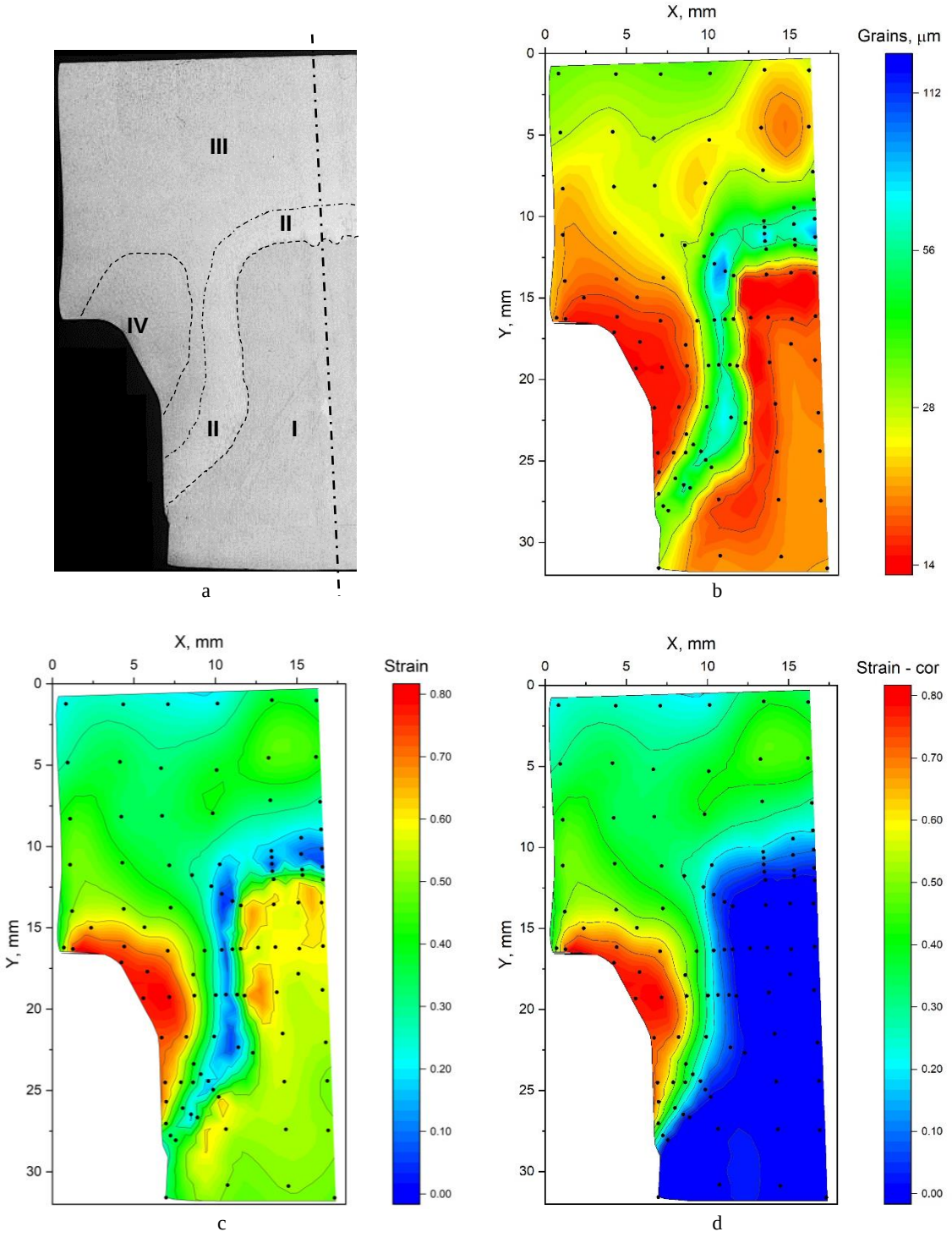

Fig. 5. Grain size in the longitudinal half-section of the extruded element: a – grain size zones; b – mean grain diameter; c – strain values; d – strain values – corrected (black dots on figures represent the position of grain diameter measurement or strain calculation)

The characteristic microstructures in the different zones of the extruded element are given in Fig. 6. The microstructure of zone I consists of small ferritic grains and strings of localized carbides island, Fig. 6a. In Fig. 6b, the boundary between zone I and II is shown, where the sudden transition from small to large grains could be observed. Furthermore, the islands of carbides in zone II are not any more localized, that is carbides are more dispersed through ferritic grains compared to zone I. Zone III has average size ferritic grains and similarly to zone II has dispersed carbides, also, Fig. 6 c. In zone IV, the strings of carbides follow the material flow, and appear highly deformed. However, the ferritic grains in zone IV are recrystallized and show no deformation. The size of grains in this zone is the smallest.

The deformation could be further assessed through the appearance of nonmetallic inclusions, Fig. 7. In zone I, where extrusion of materials prevails, nonmetallic inclusions have an elongated appearance in a matrix of equiaxial ferritic grains and well-defined carbide islands, Fig. 7a. On the other hand, in zone III the inclusions have a zigzag appearance due to radial flow of material caused by compression stresses, Fig. 7b. Also, the zigzag appearance is noticeable for the strings of carbides, and they become more dispersed in the matrix. In both cases, inclusions and carbides follow the material flow. Furthermore, in the zone I, a few very large grains are observed, Fig. 8. The size of these large grains is around 200 – 300 μm.

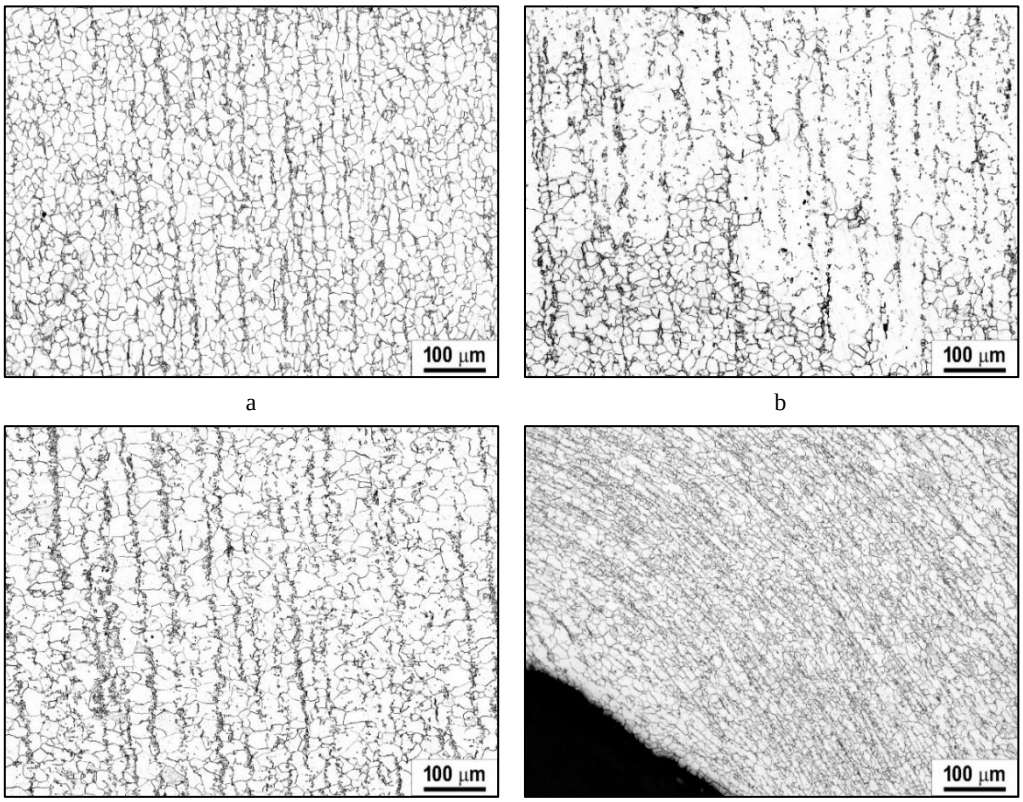

a b c d

Fig. 6. Characteristic microstructures of extruded element in the different zones: a – zone I; b – zone II; c – zone III; d – zone IV

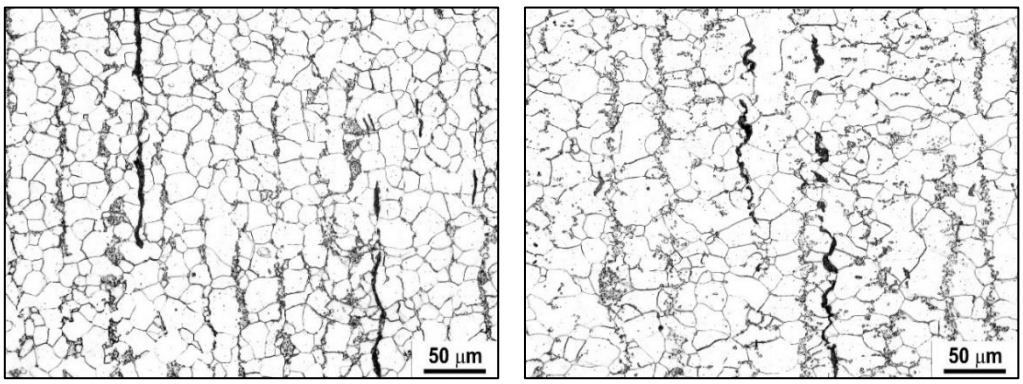

a b

Fig. 7. Deformation of nonmetallic inclusions: a – elongated inclusions – zone I; b – compressed inclusions – zone III

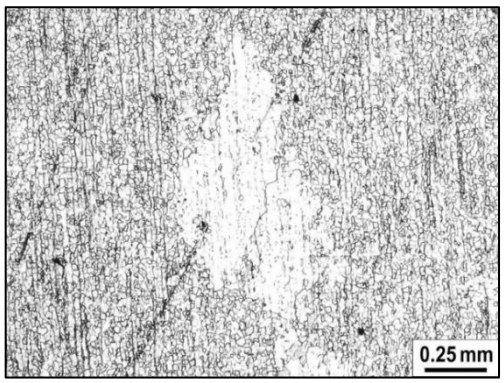

Fig. 8. Large grains in the central part of the zone I

3.3. Strain distribution

The strain values in the longitudinal half-section of the extruded element were calculated by using the calibration curve fitting Eq. 1 based on the grain size from Fig. 5 a. Results of the direct application of fitting Eq. 1 are given in Fig. 5 c, while correction of strain state based on microstructure observation in zone I is given in Fig. 5 d. Correction of strain state in zone I was needed due to overlapping grain size of starting non-deformed material (d_{av} = 18 ± 0.8 μm), and values of recrystallized grains in the same range after deformation which according to calibration curve should have strain of 0.56 to 0.63.

4. DISCUSSION

At the start of the extrusion process, when the billet is pressed by the punch, the material primarily flows through the forward extrusion die. For the given forming conditions this is the easiest way for material to flow [19 – 21]. Later, "the head" of the billet is formed, which means that material starts to flow radially, as in an upsetting process. Because the material can flow in different directions, divided flow occurs.

According to the calibration curve in zone I, where the material is extruded at the beginning of the process, and which should flow the easiest, the grains in the range of 0.18 μm are observed, thus giving strain values of around 0.6 (Fig. 5 c). However, this large deformation is not supported by microstructure observations where elongated inclusions and equiaxial ferritic grains with well-defined carbide islands are observed (Fig. 7 a). Furthermore, in this zone, a few very large grains are observed as shown in Fig. 8. The size of these grains corresponds to a strain of 0.01 to 0.02, according to the calibration curve. These values are outside the curve data range; thus, the strain could be only approximately estimated. Nevertheless, those large grains indicate that in zone I the deformation is very small, and that for this material and testing conditions a strain of around 0.02 is necessary to achieve minimum accumulated deformation energy for recrystallization to start.

All those microstructure observations indicate that in zone I there was no significant deformation. In this zone the starting grains flowed freely into the die opening. For that reason, in Fig. 5 d, a correction of the strain values in the extruded element is given. The correction is necessary for the zones where the starting grain size overlaps with recrystallized deformed grains. In the case of overlapping grain sizes, microstructure analysis must be performed as it indicates and separates zones with and without deformation.

To avoid the correction, the grain size of the initial structure (when the deformation is 0) should be sufficiently large not to overlap with any of the recrystallized grain, as was the case with single-phase material in other works [17, 18]. However, in this case of two-phase material (or two micro-constituents), this overlap was not a problem, because, even if the grain size for different strain values was the same, the difference in the microstructure indicates whether the material was deformed or not. The sufficiently large starting grains may be achieved with adequate heat treatment (usually with a prolonged time of recrystallization).

After correction (Fig. 5 d) it can be seen that zone I represents a zone of free material flow without significant deformation. Zone II represents the transition region where deformation gradually increases from low strain values $\varphi < 0.04$ observed in zone I to strain values $\varphi > 0.20$ in zone III. In zone III strains are in the range of 0.20 up to 0.45. The highest strain values are present in zone IV, from 0.45 up to 0.80. Those high values of strain are due to friction between the extruded element and the slope of the die. Friction influences the material flow, and creates a zone of high strain values in the shape of a semicircle. The size and shape of zone IV influence the contour of transition zone II and non-deformed zone I; in the lower part those zones are under 45°angle, while in the middle part contour is vertical.

5. CONCLUSIONS

In this paper, an experimental metallographic method for the determination of a strain state in a low carbon extruded element which consists of two micro-constituents (i.e., ferrite and pearlite) is presented.

The method is based on the measurement of the grain size and its correlation to strain by use of a calibration curve. Furthermore, it is shown that observation of carbides and nonmetallic inclusions morphology should be further utilized to better distinguish different deformation zones and material flow.

In the middle part of the element, material flows freely through the die opening without significant deformation. From this zone, strain gradually increases, reaching the highest value at the contact surface of the die slope. The top part flows radially having intermediate values of strain.

The strain state revealed in this way could be valuable information, for further process analysis, stress state, and process parameter determination. Additionally, it could be a helpful tool for potential critical stress sites indication.

It could be summarized that this experimental, metallographic method gives reliable information on strain distribution within extruded elements, revealing different deformations zones. Furthermore, this metallographic method, in the case of two-phase (or two micro-constituents) material, utilizing the grain size, and the deformation of carbides and nonmetallic inclusions, effectively provides the view of material flow for the analyzed stage of element extrusion.

Acknowledgments

This research has been supported by the Ministry of Science, Technological Development and Innovation through project no. 451-03-47/2023-01/200156 "Innovative scientific and artistic research from the Faculty of Technical Sciences, Novi Sad, Serbia, activity domain".

REFERENCES

1. **Lumelskyj, D., Rojek, J., Tkocz, M.** Detection of Strain Localization in Numerical Simulation of Sheet Metal Forming *Archives of Civil and Mechanical Engineering* 18 2018: pp. 490 – 499. https://doi.org/10.1016/j.acme.2017.08.004
2. **Gomez-Marquez, D., Ledesma-Orozco, E., Hino, R., Aguilera-Gomez, E., Korpała, G., Prahl, U.** Numerical Study on the Hot Compression Test for Bulk Metal Forming Application *SN Applied Sciences* 4 (220) 2022: pp. 1 – 16. https://doi.org/10.1007/s42452-022-05093-x
3. **Ding, K.Z., Qin, Q.H., Cardew-Hall, M.** Substepping Algorithms with Stress Correction for the Simulation of Sheet Metal Forming Process *International Journal of Mechanical Sciences* 49 (11) 2007: pp. 1289 – 1308. https://doi.org/10.1016/j.ijmecsci.2007.03.010
4. **Eom, J.G., Son, Y.H., Jeong, S.W., Ahn, S.T., Jang, S.M., Yoon, D.J., Joun, M.S.** Effect of Strain Hardening Capability on Plastic Deformation Behaviors of Material During Metal Forming *Materials & Design* 54 2014: pp. 1010 – 1018. https://doi.org/10.1016/j.matdes.2013.08.101
5. **Sun, L., Cai, Z., He, D., Li, L.** Aluminum Alloy Sheet-Forming Limit Curve Prediction Based on Original Measured Stress–Strain Data and Its Application in Stretch-Forming Process *Metals* 9 (10) 1129 2019: pp. 1 – 20. https://doi.org/10.3390/met9101129
6. **Liang, W., Wei, T., Yang, X.** Constitutive Model of Thin Metal Sheet in Bulging Test Considering Strain Gradient Hardening *Materials Science (Medžiagotyra)* 26 (4) 2020: pp. 415 – 425. https://matsc.ktu.lt/index.php/MatSc/article/view/22201
7. **Tabor, D.** The Hardness of Metals, Oxford University Press, London, 1951: pp. 67 – 83.
8. **Sundararajan, G., Tirupataiah, Y.** The Hardness-Flow Stress Correlation in Metallic Materials *Bulletin of Materials Science* 17 1994: pp. 747 – 770. https://doi.org/10.1007/BF02757555
9. **Alves, M.L., Rodrigues, J.M.C., Martins, P.A.F.** Cold Forging of Gears: Experimental and Theoretical Investigation *Finite Elements in Analysis and Design* 37 2001: pp. 549 – 558. https://doi.org/10.1016/S0168-874X(00)00063-9
10. **Zhang, P., Li, S.X., Zhang, Z.F.** General Relationship Between Strength and Hardness *Materials Science and Engineering: A* 529 2011: pp. 62 – 73. https://doi.org/10.1016/j.msea.2011.08.061
11. **Peng, Y., Wu, C., Gan, J., Dong, J.** Characterization of Heterogeneous Constitutive Relationship of the Welded Joint Based on the Stress-Hardness Relationship Using Micro-Hardness Tests *Construction and Building Materials* 202 2019: pp. 37 – 45 https://doi.org/10.1016/j.conbuildmat.2018.12.218
12. **Rudnytskyj, A., Varga, M., Krenn, S., Vorlaufer, G., Leimhofer, J., Jech, M., Gachot, C.** Investigating the Relationship of Hardness and Flow Stress in Metal Forming *International Journal of Mechanical Sciences* 232 (107571) 2022: pp. 1 – 17. https://doi.org/10.1016/j.ijmecsci.2022.107571
13. **Gonzalez, M.M., Lutes, N.A., Fischer, J.D., Woodside, M.R., Bristow, D.A., Landers, R.G.** Analysis of Geometric Accuracy and Thickness Reduction in Multistage Incremental Sheet Forming Using Digital Image Correlation *Procedia Manufacturing* 34 2019: pp. 950 – 960. https://doi.org/10.1016/j.promfg.2019.06.105
14. **Farahani, B.V., Belinha, J., Amaral, R., Tavares, P.J., Moreira, P.** A Digital Image Correlation Analysis on a Sheet AA6061-T6 Bi-Failure Specimen to Predict Static Failure *Engineering Failure Analysis* 90 2018: pp. 179 – 196. https://doi.org/10.1016/j.engfailanal.2018.03.011
15. **Mashiwa, N., Furushima, T., Manabe, K.** Novel Non-Contact Evaluation of Strain Distribution Using Digital Image Correlation with Laser Speckle Pattern of Low Carbon Steel Sheet *Procedia Engineering* 184 2017: pp. 16 – 21. https://doi.org/10.1016/j.proeng.2017.04.065
16. **Agirre, J., Galdos, L., de Argandoña, E.S., Mendiguren, J.** Hardening Prediction of Diverse Materials Using the Digital Image Correlation Technique *Mechanics of Materials* 124 2018: pp. 71 – 79. https://doi.org/10.1016/j.mechmat.2018.05.007
17. **Oyekanmi, B.O., Hughes, T.A., Bramley, A.N.** A Microstructural Evaluation Technique for Deformation Studies in Metal Forming Processes *Journal of Materials Processing Technology* 21 1990: pp. 75 – 89. https://doi.org/10.1016/0924-0136(90)90031-O
18. **Skakun, P., Rajnovic, D., Janjatovic, P., Balos, S., Shishkin, A., Novak, P., Sidjanin, L.** Metallographic Determination of Strain Distribution in Cold Extruded Aluminum Gear-Like Element *Metals* 10 (589) 2020: pp. 1 – 11. https://doi.org/10.3390/met10050589
19. **Kuzman, K., Pfeifer, E., Bay, N., Hunding, J.** Control of Material Flow in a Combined Backward Can – Forward Rod Extrusion *Journal of Materials Processing Technology* 60 (1 – 4) 1996: pp. 141 – 147. https://doi.org/10.1016/0924-0136(96)02319-9
20. **Fereshteh-Saniee, F., Pillinger, I., Hartley, P.** Friction Modelling for the Physical Simulation of the Bulk Metal Forming Processes *Journal of Materials Processing Technology* 153 – 154 2004: pp. 151 – 156. https://doi.org/10.1016/j.jmatprotec.2004.04.217
21. **Hu, C., Yin, Q., Zhao, Z.** A Novel Method for Determining Friction in Cold Forging of Complex Parts Using a Steady Combined Forward and Backward Extrusion Test *Journal of Materials Processing Technology* 249 2017: pp. 57 – 66. https://doi.org/10.1016/j.jmatprotec.2017.06.001